Am J Physiol Heart Circ Physiol 285: H541–H548, 2003.
First published April 24, 2003; 10.1152/ajpheart.01142.2002.

Oxidative capacity in failing hearts

Guangrong Gong, Jingbo Liu, Peihua Liang, Tao Guo, Qingsong Hu, Ko Ochiai, Mingxiao Hou, Yun Ye, Xiaoyun Wu, Abdul Mansoor, Arthur H. L. From, Kamil Ugurbil, Robert J. Bache, and Jianyi Zhang

Departments of Medicine and Radiology and Center for Magnetic Resonance Research, University of Minnesota, Minneapolis, Minnesota 55455

Submitted 23 December 2002; accepted in final form 4 April 2003

Gong, Guangrong, Jingbo Liu, Peihua Liang, Tao Guo, Qingsong Hu, Ko Ochiai, Mingxiao Hou, Yun Ye, Xiaoyun Wu, Abdul Mansoor, Arthur H. L. From, Kamil Ugurbil, Robert J. Bache, and Jianyi Zhang. Oxidative capacity in failing hearts. *Am J Physiol Heart Circ Physiol* 285: H541–H548, 2003. First published April 24, 2003; 10.1152/ajpheart.01142.2002.—Although high-energy phosphate metabolism is abnormal in failing hearts [congestive heart failure (CHF)], it is unclear whether oxidative capacity is impaired. This study used the mitochondrial uncoupling agent 2,4-dinitrophenol (DNP) to determine whether reserve oxidative capacity exists during the high workload produced by catecholamine infusion in hypertrophied and failing hearts. Left ventricular hypertrophy (LVH) was produced by ascending aortic banding in 21 swine; 9 animals developed CHF. Basal myocardial phosphocreatine (PCr)/ATP measured with ^{31}P NMR spectroscopy was decreased in both LVH and CHF hearts (corresponding to an increase in free [ADP]), whereas ATP was decreased in hearts with CHF. Infusion of dobutamine and dopamine (each 20 $\mu g \cdot kg^{-1} \cdot min^{-1}$ iv) caused an approximate doubling of myocardial oxygen consumption ($M\dot{V}O_2$) in all groups and decreased PCr/ATP in the normal and LVH groups. During continuing catecholamine infusion, DNP (2–8 mg/kg iv) caused further increases of $M\dot{V}O_2$ in normal and LVH hearts with no change in PCr/ATP. In contrast, DNP caused no increase in $M\dot{V}O_2$ in the failing hearts; the associated decrease of PCr/ATP suggests that DNP decreased the mitochondrial proton gradient, thereby causing ADP to increase to maintain adequate ATP synthesis.

heart failure; left ventricular hypertrophy; mitochondria; high-energy phosphates; nuclear magnetic resonance

IN NORMAL MYOCARDIUM, it is unclear whether peak O_2 utilization is ultimately limited by maximal oxidative ATP synthetic capacity or by the maximal capacities of the myosin and other ATPases to utilize ATP. In failing myocardium, abnormalities of excitation-contraction coupling as well as downregulation of β-adrenergic receptors and the downstream adenylyl cyclase system (25) make it even more difficult to determine whether ATP synthetic capacity limits contractile performance. Hence, the hypothesis that primary "energy starvation" limits function in heart failure (14) remains to be rigorously tested in vivo despite evidence that left ventricular (LV) hypertrophy (LVH) and congestive heart failure (CHF) are associated with abnormalities of myocardial energy metabolism (2, 21, 22, 38, 39).

Consequently, the present study was performed to determine whether administration of a classical mitochondrial uncoupling agent [2,4-dinitrophenol (DNP)] could further increase myocardial oxygen consumption ($M\dot{V}O_2$) in hearts with compensated LVH or overt cardiac failure that were already functioning at a high work state produced by catecholamine stimulation. DNP accelerates intramitochondrial metabolism proximal to ATP synthase by decreasing the proton gradient across the inner mitochondrial membrane (17, 30). In response to DNP, $M\dot{V}O_2$ increases in concert with intermediary metabolism and electron transport activity to maintain the mitochondrial proton gradient that drives ATP synthesis (15, 17, 30). Although it is unlikely that DNP can define the maximal oxygen utilization capacity in the intact heart (8), it can be used to determine whether there is a reserve capacity of the reaction sequences that generate the mitochondrial proton gradient required to support ATP synthase activity. We hypothesized that if the capacities of the energetic reactions proximal to ATP synthase constrained mechanical performance during high work states, then DNP would not cause a further increase of $M\dot{V}O_2$ and might cause deterioration of mechanical performance and myocardial high-energy phosphate (HEP) content. Measurements of myocardial HEP levels were made with ^{31}P NMR spectroscopy. Because of concerns that abnormalities of perfusion or diffusion might limit oxygen delivery and thereby impair respiratory rates in the hypertrophied or failing hearts, myocyte oxygenation was assessed using ^{1}H NMR spectroscopy.

METHODS

Experiments were performed in accordance with the "Position of the American Heart Association on Research Animal Use," adopted November 11, 1984, and protocols were approved by the Animal Care Committee of the University of Minnesota.

Production of LVH. Sixteen Yorkshire pigs at ~45 days of age were anesthetized with pentobarbital sodium (25–30

Address for reprint requests and other correspondence: J. Zhang, Cardiovascular Div., Dept. of Medicine, Univ. of Minnesota Medical School, Mayo Mail Code 508, UMHC, Minneapolis, MN 55455 (E-mail: zhang047@umn.edu).

The costs of publication of this article were defrayed in part by the payment of page charges. The article must therefore be hereby marked "*advertisement*" in accordance with 18 U.S.C. Section 1734 solely to indicate this fact.

mg/kg iv), intubated, and ventilated with a respirator. A right thoracotomy was performed in the third intercostal space, and the ascending aorta, ~1.5 cm above the aortic valve, was mobilized and encircled with a polyethylene band 2.5 mm in width. While LV and distal aortic pressures were simultaneously measured, the band was tightened until a 70-mmHg peak systolic pressure gradient was achieved across the narrowing. The chest was then closed, the pneumothorax was evacuated, and the animals were allowed to recover. LVH occurred progressively as the area of aortic constriction remained fixed in the face of normal body growth. Two months after being banded, animals were returned to the laboratory for study.

Experimental preparation. Ten normal pigs and twenty-one pigs with LVH were premedicated with morphine sulfate (l mg/kg sc) and anesthetized with pentobarbital (30 mg/kg iv, followed by an infusion of 4 $mg \cdot kg^{-1} \cdot h^{-1}$). A smaller dose of pentobarbital (~20 mg/kg iv) was used for animals with CHF to prevent loss of animals from general anesthesia. Animals were intubated and ventilated with a respirator with supplemental oxygen; arterial blood gases and pH were maintained within the physiological range. A polyvinyl chloride catheter (3.0 mm outer diameter) filled with heparin-saline was introduced into the right femoral artery and advanced into the ascending aorta. A left thoracotomy was performed in the fifth intercostal space, and the heart was suspended in a pericardial cradle. A heparin-saline-filled catheter was introduced into the LV through the apical dimple and secured with a purse-string suture. A similar catheter was placed into the left atrium through the atrial appendage. A catheter was also introduced into the anterior coronary vein via the right atrial appendage. An NMR surface coil was sutured to the anterior LV wall overlying the region perfused by the left anterior descending coronary artery. The surface coil was constructed of a single turn of copper wire and incorporated a 33-pF capacitor; surface coils were 28 mm in diameter. The surface coil leads were connected to a balanced-tuned circuit external and perpendicular to the thoracotomy incision. The pericardial cradle was released, and the heart was allowed to assume its normal position. The animals were then placed in a Lucite cradle and positioned within the magnet. Arterial blood gases were measured every 15 min, and the respirator was adjusted to maintain the P_{O_2}, P_{CO_2}, and pH in the physiological range.

Myocardial blood flow. Myocardial blood flow was measured with microspheres (15 μm in diameter) labeled with ^{141}Ce, ^{51}Cr, ^{95}Nb, ^{85}Sr, or ^{46}Sc (NEN; Boston, MA) as previously described (3). Blood flow was expressed as milliliters per minute per gram of myocardium.

^{31}P NMR spectroscopic technique. Our NMR spectroscopic methods have been described in detail previously (3, 10, 11, 29). Measurements were performed in a 40-cm bore 4.7-T magnet interfaced with a SISCO (Spectroscopy Imaging Systems; Fremont, CA) computer console. The LV pressure signal was used to gate NMR data acquisition to the cardiac cycle, whereas respiratory gating was achieved by triggering the ventilator to the cardiac cycle between data acquisitions. ^{31}P and ^{1}H NMR frequencies were 81 and 200.1 MHz, respectively. Spectra were recorded in late diastole with a pulse repetition time of 6–7 s. This repetition time allowed full relaxation for ATP and P_i resonances and ~90% relaxation of the phosphocreatine (PCr) resonance; PCr resonance intensities were corrected for this minor saturation. Radiofrequency transmission and signal detection were performed with a 28-mm-diameter surface coil dually tuned for both ^{1}H and ^{31}P measurements. A capillary containing 15 μl of 3 M phosphonoacetic acid was placed at the coil center to serve as a reference. The proton signal from water was used to homogenize the magnetic field and adjust the position of the animal in the magnet so that the coil was at or near the magnet and gradient isocenters. Spectra were obtained with the image-selected in vivo spectroscopy (ISIS) method, which defined a column 1.8×1.8 cm^2 perpendicular to the LV wall. ^{31}P signal excitation was achieved with a 90°, adiabatic, B_1-insensitive, BIR-4 pulse. All chemical shifts were measured relative to the PCr peak, which was assigned a chemical shift of −2.55 ppm relative to 85% phosphonoacetic acid at 0 ppm.

Resonance intensities were quantified using integration routines provided by SISCO software. The ATPγ resonance was used for ATP determination. Because data were acquired with the transmitter frequency positioned between the ATPγ and PCr resonances, off resonance effects on these peaks were virtually nonexistent. Numerical values for PCr and ATP were expressed as ratios of PCr to ATP (PCr/ATP). P_i levels were measured as changes from baseline values (ΔPi) using integrals obtained in the region covering the P_i resonance and are presented as ΔP_i/PCr. ADP levels in each group were calculated using chemically measured total creatine and ATP levels, and ^{31}P NMR determined PCr and intracellular pH levels as previously described (16).

^{1}H NMR spectroscopic technique. Determination of deoxymyoglobin (Mb-δ) using the ^{1}H NMR method has previously been reported in detail (5, 38). In brief, radiofrequency transmission and signal detection were performed with the dually tuned 28-mm-diameter surface coil. A single-pulse collection sequence with a frequency-selective gauss excitation pulse (1 ms) was used to selectively excite the N-δ proton signal of the proximal histidine in Mb-δ. A short repetition time (25 ms) was used due to the short T_1 of Mb-δ. Each spectrum is acquired in 5 min (10,000 free induction decays). Although the short T_1 of Mb-δ and fast acquisition prevent gating to the cardiac cycle, the signal loss due to motion was negligible due to the inherently broad line width of the Mb-δ peak.

Hemodynamic measurements. Aortic and LV pressures were monitored with pressure transducers positioned at the midchest level. Data were recorded on an eight-channel direct writing recorder (Coulbourne Instrument; Lehigh Valley, PA). LV pressure was recorded at normal and high gain for measurement of end-diastolic pressure.

Experimental protocol. Hemodynamic measurements and NMR spectra were first obtained under basal conditions. Midway through the 10-min NMR data-acquisition period, a microsphere injection was performed for determination of myocardial blood flow. After baseline data were obtained, dobutamine and dopamine were infused simultaneously (each 20 $\mu g \cdot kg^{-1} \cdot min^{-1}$ iv) to induce a high cardiac work state. After ~10 min was allowed to achieve a steady state, all measurements were repeated. After completion of data acquisition, while the dobutamine and dopamine infusion continued, four sequential 5-min infusions of DNP (each 2 mg/kg iv) were given; all measurements were repeated after a 10- to 15-min stabilization period after the first infusion (2 mg/kg) and after the final infusion (cumulative dose 8 mg/kg). Microspheres were administered for measurement of myocardial blood flow during baseline conditions, during catecholamine infusion, and during the DNP infusion.

Tissue preparation. With the use of a forceps precooled to −70°C, at the end of the experiment, an epicardial biopsy was taken from five normal, four LVH, and four CHF ventricles for subsequent analysis of ATP and creatine content using HPLC techniques (31). The heart was then fixed in 10% buffered formalin. The myocardium beneath the surface coil was sectioned into three transmural layers from epicardium

Table 1. *Anatomic data*

	n	Body Weight, kg	LV Weight, g	RV Weight, g	LV Weight/Body Weight, g/kg	RV Weight/Body Weight, g/kg
Normal	12	38.0 ± 2.2	91.8 ± 6.6	33.4 ± 1.7	2.44 ± 0.2	0.90 ± 0.05
LVH	12	41.7 ± 3.7	151.1 ± 15.7*	51.8 ± 4.3*	3.68 ± 0.23*	1.34 ± 0.16*
CHF	9	36.8 ± 4.7	167.9 ± 18.6*	61.3 ± 5.8*	4.91 ± 0.58*†	1.88 ± 0.32*

Values are means ± SE; *n,* no. of pigs. LVH, left ventricular (LV) hypertrophy; CHF, congestive heart failure; RV, right ventricular. *$P <$ 0.01 vs. normal; †$P < 0.05$ vs. LVH.

to endocardium, weighed on an analytic balance, and placed into vials for counting of radioactivity. Similar specimens were obtained from the lateral and posterior LV wall to insure that the sample from beneath the surface coil was typical of the entire LV.

Data analysis. Numerical values for PCr and ATP during each experimental condition were expressed as PCr/ATP. $M\dot{V}O_2$ was calculated from the measured blood flows and the difference in O_2 content between aortic and anterior coronary vein blood samples. Hemodynamic data were measured from the chart recordings. Hemodynamic, biochemical, and blood flow data were analyzed with one-way ANOVA with replications. A value of $P < 0.05$ was required for significance. When the ANOVA yielded a significant result, individual comparisons were made using the method of Scheffé. Data are reported as means ± SE.

RESULTS

Animal model. Nine of twenty-one pigs with aortic banding developed CHF as evidenced by ascites (range 100–2,000 ml). The remaining 12 pigs with aortic banding formed the compensated LVH group. The anatomic data are summarized in Table 1. The ratio of LV weight to body weight was increased by 51% in hearts with LVH ($P < 0.05$ vs. control) and increased by 101% in hearts with CHF ($P < 0.05$ vs. LVH). The ratio of right ventricular weight to body weight was increased in both LVH and CHF groups ($P < 0.05$). Figure 1 shows a typical short-axis section of a normal LV (Fig. 1*A*) with a wall thickness of 0.8 cm compared with a typical LVH heart with concentric hypertrophy (Fig. 1*B*) in which wall thickness was 2.0 cm and the cavity size was decreased.

Hemodynamic data. Hemodynamic data are shown in Table 2. At baseline, LV systolic pressure and the rate-pressure product (RPP) were significantly higher in hearts with aortic stenosis than in normal hearts (Table 2). LV end-diastolic pressure was significantly increased only in hearts with CHF. In all three groups, heart rate, LV systolic pressure, and RPP increased significantly during catecholamine stimulation. During high-dose DNP infusion, RPP increased significantly in the LVH and CHF animals but not in the normal group.

Myocardial blood flow and oxygen consumption data. Mean myocardial blood flow and the transmural distribution of perfusion were similar in normal, LVH, and CHF hearts at baseline (Table 3). Myocardial blood

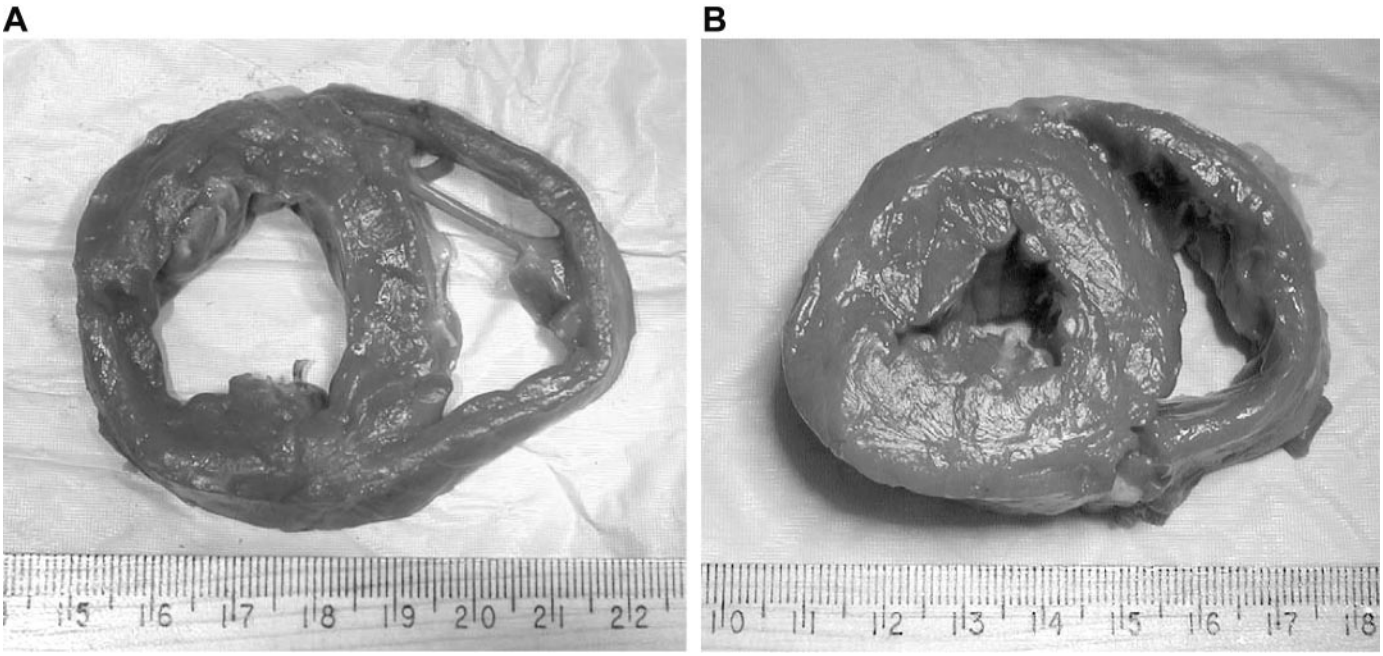

Fig. 1. Short-axis view of the mid-left ventricle (LV) from a 26-kg normal pig (*A*) and from a 27-kg pig with compensated LV hypertrophy (LVH) secondary to aortic banding (*B*). The ratio of the LV cavity diameter to wall thickness is markedly decreased in the heart with LVH.

Table 2. *Hemodynamic data*

	n	Heart Rate, beats/min	Mean Aortic Pressure, mmHg	LV Systolic Pressure, mmHg	LV End-Diastolic Pressure, mmHg	Rate-Pressure Product, 1,000·(mmHg·beats·min^{-1})
Baseline						
Normal	12	112 ± 7	77 ± 1	112 ± 7	7 ± 1	12.80 ± 1.43
LVH	12	123 ± 3	90 ± 1	136 ± 5*	10 ± 1	16.42 ± 0.33*
CHF	9	131 ± 10	87 ± 9	142 ± 13*	17 ± 3*	18.53 ± 1.92*
DbDp						
Normal	12	171 ± 10†	91 ± 5	186 ± 9†	7 ± 1	31.65 ± 2.45†
LVH	12	187 ± 14†	96 ± 8	208 ± 17†	10 ± 2	39.49 ± 5.17†
CHF	9	177 ± 17†	87 ± 8	210 ± 32†	18 ± 3*	38.47 ± 6.79†
DNP (2 mg/kg iv)						
Normal	12	186 ± 13	84 ± 6	194 ± 10	7 ± 1	36.36 ± 3.30
LVH	12	183 ± 10	90 ± 7	241 ± 22	13 ± 2*	43.20 ± 3.11
CHF	9	184 ± 21	87 ± 8	210 ± 33	19 ± 3*	41.59 ± 9.41
DNP (8 mg/kg iv)						
Normal	12	193 ± 13	80 ± 4	174 ± 9	7 ± 1	33.54 ± 3.00
LVH	12	201 ± 13	90 ± 8	235 ± 15	13 ± 2*	46.39 ± 1.97*‡
CHF	9	208 ± 21	82 ± 5	230 ± 32*	20 ± 10*	47.84 ± 7.60*‡

Values are means ± SE; *n,* no. of pigs. DbDp, dobutamine and dopamine (each 20 mg·kg^{-1}·min^{-1}); DNP, 2,4-dinitrophenol. *$P < 0.05$ vs. normal; †$P < 0.01$ vs. baseline; ‡$P < 0.05$ vs. DbDp.

flow and $M\dot{V}O_2$ increased significantly in all three groups during catecholamine infusion. $M\dot{V}O_2$ increased further in the normal and LVH groups during DNP infusion but not in the CHF group.

HEP measurements. HEP data are summarized in Table 4. In normal animals, ^{31}P spectra recorded during the control period were characterized by high PCr/ATP. Basal PCr/ATP was significantly decreased in hearts with LVH and further decreased in CHF hearts (Table 4, $P < 0.05$ vs. normal). P_i was too low to identify at the signal-to-noise ratio of the spectra under basal conditions in any group. Infusion of dopamine-dobutamine caused significant reductions of PCr/ATP in normal and LVH hearts without a significant change in the already low PCr/ATP in CHF hearts. Catecholamine infusion was associated with the appearance of a P_i resonance in all three groups of animals. As shown in Table 4, the addition of DNP to dobutamine-dopamine caused no further change of PCr/ATP in the normal and LVH groups. However, in the animals with CHF, DNP caused a significant further decrease of PCr/ATP, from 1.61 ± 0.06 to 1.47 ± 0.11 ($P < 0.05$). In the normal animals, the addition of DNP during catecholamine infusion caused no change in ΔP_i/PCr. In contrast, in both the LVH and CHF groups, the addition of DNP resulted in significant increases of ΔP_i/PCr (Table 4). As shown in Table 5, both ATP and total creatine levels (chemically measured) were reduced in the CHF group, whereas calculated [ADP] was significantly increased in both the LVH and CHF groups.

Mb-δ measurements. No Mb-δ resonance was observed in any group under any of the experimental con-

Table 3. *Myocardial blood flow and oxygen consumption data*

		Myocardial Blood Flow, ml·min^{-1}·g^{-1}				Mean Myocardial Blood Flow, ml·min^{-1}·g^{-1}	Coronary Venous Oxygen Pressure, Torr	AV Oxygen Difference, ml O_2/100 ml	$M\dot{V}O_2$, ml·min^{-1}·100 g^{-1}
	n	Epi	Mid	Endo	Endo/Epi				
Baseline									
Normal	12	0.94 ± 0.12	1.02 ± 0.14	1.00 ± 0.15	1.08 ± 0.08	0.99 ± 0.14	23.5 ± 2.1	12.12 ± 0.60	11.84 ± 1.78
LVH	12	1.00 ± 0.12	1.04 ± 0.10	1.06 ± 0.10	1.09 ± 0.05	1.04 ± 0.11	24.4 ± 1.3	12.61 ± 0.55	13.72 ± 1.64
CHF	9	1.10 ± 0.13	1.27 ± 0.17	1.23 ± 0.14	1.13 ± 0.06	1.20 ± 0.14	23.1 ± 1.1	12.94 ± 0.28	15.63 ± 1.99
DbDp									
Normal	12	2.08 ± 0.21*	2.23 ± 0.23*	2.09 ± 0.25*	1.03 ± 0.10	2.13 ± 0.21*	24.0 ± 1.6	11.31 ± 0.49	23.95 ± 1.96*
LVH	12	1.87 ± 0.19*	1.88 ± 0.24*	1.92 ± 0.17*	1.01 ± 0.04	1.89 ± 0.20*	23.3 ± 1.1	12.51 ± 0.42	23.27 ± 2.76*
CHF	9	2.66 ± 0.52*	2.96 ± 0.59*	2.78 ± 0.48*	1.06 ± 0.06	2.80 ± 0.41*	21.9 ± 2.1	11.59 ± 1.00	32.10 ± 5.05*
DNP (2 mg/kg iv)									
Normal	12	1.97 ± 0.37	2.16 ± 0.43	1.92 ± 0.38	0.98 ± 0.07	2.02 ± 0.38	23.0 ± 1.7	12.15 ± 0.77	23.53 ± 2.80
LVH	12	1.84 ± 0.25	1.90 ± 0.23	1.87 ± 0.22	1.04 ± 0.05	1.87 ± 0.23	22.5 ± 2.2	13.61 ± 0.80	24.76 ± 2.50
CHF	9	2.65 ± 0.49	2.84 ± 0.61	2.56 ± 0.53	0.97 ± 0.09	2.68 ± 0.52	24.3 ± 1.8	11.56 ± 1.10	29.40 ± 8.42
DNP (8 mg/kg iv)									
Normal	12	2.97 ± 0.78	2.94 ± 0.83	2.78 ± 0.80	0.93 ± 0.05	2.89 ± 0.80	26.5 ± 0.8	12.17 ± 1.08	33.02 ± 8.02†
LVH	12	2.55 ± 0.36	2.50 ± 0.31	2.52 ± 0.33	1.00 ± 0.05	2.52 ± 0.33	21.3 ± 2.2	12.98 ± 0.55	32.33 ± 4.85†
CHF	9	2.73 ± 0.47	2.80 ± 0.54	2.78 ± 0.63	0.99 ± 0.06	2.77 ± 0.55	23.4 ± 1.7	12.26 ± 0.67	33.51 ± 6.29†

Values are means ± SE; *n,* no. of pigs. Epi, epicardium; Mid, midmyocardium; Endo, endocardium; AV, atrioventricular; $M\dot{V}O_2$, myocardial oxygen consumption. *$P < 0.05$ vs. baseline; †$P < 0.05$ vs. DbDp.

Table 4. *Myocardial high-energy phosphates*

	ΔP_i/PCr			PCr/ATP		
	Normal	LVH	CHF	Normal	LVH	CHF
n	12	12	9	12	12	9
Baseline	0	0	0	2.07 ± 0.07	1.86 ± 0.09*	1.68 ± 0.07*
DbDp	0.25 ± 0.07†	0.25 ± 0.08†	0.49 ± 0.12†	1.88 ± 0.10†	1.67 ± 0.09†	1.61 ± 0.06
DNP (2 mg/kg iv)	0.29 ± 0.11	0.27 ± 0.08	0.46 ± 0.15	1.89 ± 0.11	1.75 ± 0.09	1.47 ± 0.11‡
DNP (8 mg/kg iv)	0.35 ± 0.17	0.45 ± 0.10‡	0.72 ± 0.09‡	1.91 ± 0.16	1.68 ± 0.05	1.46 ± 0.09

Values are means ± SE; *n,* no. of pigs. PCr, phosphocreatine. *$P < 0.01$ vs. normal; †$P < 0.05$ vs. baseline; ‡$P < 0.05$ vs. DbDp.

ditions, although transient occlusion of the coronary artery supplying the area of myocardium beneath the NMR coil consistently produced a large Mb-δ resonance.

DISCUSSION

The major findings in the present study are as follows: *1*) basal state values of PCr/ATP were reduced in both groups with aortic banding (corresponding to increased free ADP), with the most severe reductions being present in the CHF group; *2*) when DNP was administered during catecholamine infusion, $M\dot{V}O_2$ increased significantly in the normal and LVH groups but not in the CHF group; and *3*) DNP had no additional effect on PCr/ATP in the normal and LVH groups but caused a significant further reduction of PCr/ATP in the CHF group. These findings suggest that near-maximal oxidative capacity had been approached during catecholamine stimulation in the CHF hearts but not in normal hearts or hearts with compensated hypertrophy.

Swine pressure-overload hypertrophy model. In the present study, a supravalvular aortic stenosis was applied in juvenile swine to produce an initial pressure gradient of ~70 mmHg across the constriction (35). The animals subsequently developed myocardial hypertrophy as the degree of aortic narrowing remained fixed in the face of normal body growth. Approximately 40% of the animals developed CHF as manifested by an increased LV end-diastolic pressure, exercise intolerance, and ascites; the increase in LV/body weight was twice as great in animals that developed CHF as in those with compensated LVH. With the use of a similar but milder degree of aortic constriction in swine, Massie et al. (19) found that a stenosis that produced a 25-mmHg pressure gradient across the aortic narrowing resulted in a 38% increase of LV mass in 6 mo with no evidence of heart failure in any of the animals. The more severe aortic narrowing makes the present model useful for study of the response of physiological and metabolic variables to severe pressure overload and the evolution to overt CHF.

Table 5. *Myocardial ATP, total creatine, and calculated free ADP levels*

	n	[ATP], μmol/g dry wt	Total [Cr], μmol/g dry wt	Free [ADP], mmol/g dry wt
Normal	6	21.9 ± 3.2	113 ± 16.5	261 ± 31
LVH	5	18.5 ± 2.6	119 ± 18.3	359 ± 36*
CHF	5	15.6 ± 3.0*	86 ± 15.1*†	347 ± 35*

Values are means ± SE; *n,* no. of pigs. *$P < 0.05$ vs. normal; †$P < 0.05$ vs. LVH.

Previous evidence of bioenergetic abnormalities in hypertrophied and failing myocardium. Myocardial PCr/ATP is decreased in patients (22) and in large and small animal models of LVH secondary to pressure and volume overload and postinfarction LV remodeling (11, 21, 23, 36, 37, 39). Furthermore, abnormalities in oxidative phosphorylation have been described in in vitro studies of failing myocardium (6, 32). Consistent with these observations, we (18, 24) recently reported that ATP synthase and adenine nucleotide translocator (ANT) protein expression is decreased in animals with CHF secondary to postinfarction remodeling or pacing-induced heart failure. In swine with moderate pressure overload produced by ascending aortic constriction, Massie et al. (19) found that basal PCr/ATP tended to be decreased in animals with LVH and that PCr/ATP decreased significantly and similarly in normal and LVH hearts during the increased cardiac work state produced by dobutamine infusion. They observed that animals with LVH had greater glucose uptake during dobutamine stimulation; however, a greater fraction of the glucose was oxidized in the LVH animals, indicated that the preference for glucose in the LVH hearts was not the result of ischemia. This finding is in agreement with the absence of Mb-δ in the present study, indicating adequate oxygen availability. Thus the animals in that study behaved similarly to the animals with compensated LVH in the present study.

Do metabolic limitations constrain myocardial function? During basal conditions, [ADP] was higher in the LVH and CHF hearts than in the normal group. This indicates that the kinetic relationship between [ADP] and the ATP synthesis rate (as indicated by $M\dot{V}O_2$) is altered in LVH and CHF myocardium (37). Altered substrate preference might contribute to the increased [ADP] in the overloaded hearts. Hypertrophied and failing hearts demonstrate increased glucose utilization (4); an increase in [ADP] has been found in perfused hearts when glucose is the sole substrate (9). Furthermore, swine hearts with CHF secondary to postinfarction LV remodeling demonstrate decreased expression of F_1F_0-ATPase and ANT1 proteins (18, 24). The increased [ADP] may reflect successful kinetic adaptation to the reduced ATP synthase and ANT1 protein expression or activity. However, the ability to increase contractile performance and oxygen consump-

tion in response to catecholamine stimulation in the present study indicates that, under basal conditions, the hypertrophied and failing hearts did have significant cytosolic and mitochondrial metabolic reserve capacity to augment the ATP synthetic rate.

During catecholamine infusion, $M\dot{V}O_2$ approximately doubled in all groups. The animals with compensated LVH tolerated the increased need for ATP synthesis during catecholamine stimulation with no greater decrease of PCr/ATP than the normal hearts, and the already low PCr/ATP in the CHF group did not decrease further. The normal $M\dot{V}O_2$ and functional responses of the CHF hearts to catecholamine stimulation were surprising given the depressed adrenergic responsiveness generally observed in failing hearts (25). It is possible that there is less downregulation of β-adrenergic receptor pathways in the present swine pressure overload model than in CHF of other etiologies. In addition, the aortic constriction appeared to contribute to the increase of RPP, because, although aortic pressure did not increase in the CHF hearts during catecholamine infusion (unlike the normal hearts in which aortic pressure did increase), LV systolic pressure did increase significantly during catecholamine infusion. In any event, the ability of the hypertrophied and failing hearts to respond to catecholamine simulation was not less than that of normal hearts.

Use of partial mitochondrial uncoupling to unmask a mitochondrial functional abnormality. The mitochondrial uncoupling agent DNP was used to examine whether mitochondrial oxidative capacity (proximal to ATP synthase) was limited in LVH or CHF hearts during catecholamine stimulation. DNP decreases the proton gradient across the mitochondrial inner membrane that is required to support ATP synthesis. This results in compensatory augmentation of mitochondrial carbon substrate and oxygen consumption to maintain the proton gradient sufficient to sustain mitochondrial function (15, 30). Thus DNP would be expected to increase $M\dot{V}O_2$ and the rates of the supporting metabolic reactions that cause electrons to be delivered to cytochrome oxidase if the rates of these reactions are not already maximal. That is, an increase of $M\dot{V}O_2$ in response to DNP administration would indicate the presence of a functional reserve proximal to ATP synthase. In the present study, DNP administered during continuing catecholamine infusion elicited a ~22% increase in $M\dot{V}O_2$ in normal hearts and in hearts with compensated LVH, indicating a reserve oxidative capacity. Furthermore, the increased $M\dot{V}O_2$ produced by DNP did not tax oxygen delivery to the myocardium, because myocardial Mb-δ remained below the level of detection. Taken together, these data indicate that during DNP infusion, there was no limitation of cytosolic oxygen availability and that the reserve oxidative capacity (i.e., beyond the level reached during catecholamine administration alone) was present in normal hearts and in hearts with compensated hypertrophy.

In contrast to the normal hearts and hearts with compensated hypertrophy, in the failing hearts administration of DNP during catecholamine infusion caused no further increase in $M\dot{V}O_2$. Furthermore, DNP caused a significant decrease of the already low PCr/ATP. DNP tended to increase RPP in all groups of animals, and this was significant in the LVH and CHF groups during the high dose. This increase in cardiac work may have contributed to the increased $M\dot{V}O_2$ in the normal and LVH groups as well as to the decrease in PCr/ATP in the failing hearts. The failure of $M\dot{V}O_2$ to increase in response to DNP in the CHF group suggests that the maximal capacity to utilize O_2 had been approached during catecholamine stimulation. The fall of PCr/ATP would be consistent with this view and suggests that a compensatory increase of [ADP] occurred because respiration was not able increase to compensate for the increased proton leak across the inner mitochondrial membrane caused by DNP (30). Alternatively, it is possible that $M\dot{V}O_2$ failed to increase during DNP because the failing hearts had already become partially uncoupled during the high workload produced by catecholamine administration. Although the absolute increase in $M\dot{V}O_2$ in response to dobutamine-dopamine was greater in the CHF hearts, the relative increase (compared with the baseline value) was similar in normal (+102%) and CHF hearts (+105%) but tended to be less in LVH hearts (+70%). The mechanism for the greater $M\dot{V}O_2$ per gram of myocardium during baseline conditions in the aortic banded animals is uncertain, although we (1) have previously observed that $M\dot{V}O_2$ was also significantly higher in dogs with LVH secondary to aortic banding studied during awake conditions. It is likely that the increase in $M\dot{V}O_2$ during dobutamine-dopamine in the CHF hearts brought them closer to abolishing their respiratory reserve compared with the normal hearts or the hearts with compensated LVH.

Our findings are in agreement with previous in vitro studies that have demonstrated that the maximal oxidative capacity of mitochondria (33) or skinned fibers from failing myocardium is decreased compared with normal myocardium (32). However, the current data indicate that such abnormalities are not sufficiently severe to constrain in vivo performance at the moderately high work states induced by catecholamine administration. Thus during basal conditions and with moderate increases of cardiac workload bioenergetic abnormalities in failing myocardium were not functionally limiting, and the decreased contractile performance was likely the result of primary contractile abnormalities of the myocytes (34) as well as an unfavorable chamber geometry (13). Therefore, during catecholamine administration, the rate of ATP expenditure, rather than limitation of mitochondrial function, appeared to determine $M\dot{V}O_2$ in all groups of hearts. However, the DNP data suggest that maximal $M\dot{V}O_2$ had been approached in the CHF group during catecholamine infusion. Calculations based on study of the oxidative capacity of isolated mitochondria (18) suggest that the maximal oxygen consumption capacity of

normal swine myocardium should be ~24.3 μmol·g wet wt^{-1}·min^{-1} or ~54 ml·100 g wet wt^{-1}·min^{-1} (20). Because this value is nearly twice the maximum $M\dot{V}O_2$ values achieved in the present study, a significant reduction of mitochondrial capacity in the LVH group might not have been detected with the present experimental protocol.

DNP causes increased local metabolic demands, which in turn result in metabolic vasodilation of the resistance vessels. In peripheral tissues, DNP causes a marked increase in oxygen extraction. However, in the porcine hearts in the present study, DNP caused no significant change in coronary venous oxygen tension, indicating no consistent change in myocardial oxygen extraction. If DNP had acted as a primary coronary vasodilator, then one would have expected decreased oxygen extraction by the heart with an increase in coronary venous oxygen tension. Conversely, if the increase in coronary flow was the result of an increase in oxygen demands, then one might have expected a decrease in coronary venous oxygen tension, because presumably an error signal would be required to elicit metabolic vasodilation. This did not occur. The possibility remains that DNP caused metabolic vasodilation but that oxygen was not the mediator of that response; rather, some other metabolic signal during DNP could have caused vasodilation. It is of interest that there is a difference in the response of coronary venous oxygen tension between dogs and swine during exercise. Whereas dogs show a marked decrease in coronary venous P_{O_2} during exercise, swine do not, apparently because of feedforward control of the coronary circulation by the adrenergic nervous system (7). It is possible that adrenergic activation during DNP infusion similarly caused some degree of coronary vasodilation that prevented an increase in myocardial oxygen extraction in the present study.

The absence of myocardial myoglobin desaturation indicates that the increased oxygen utilization during catecholamine infusion and DNP administration did not exceed the ability to deliver oxygen. The inability to detect Mb-δ with the ^{1}H NMR technique indicates that myocyte P_{O_2} values were >15 mmHg, far above the Michaelis-Menten constant value for O_2 with respect to cytochrome oxidase (38). However, the $M\dot{V}O_2$ values measured during maximal catecholamine stimulation are substantially lower than the $M\dot{V}O_2$ levels that have been measured in normal hearts during heavy exercise (1). Furthermore, DNP-induced increases of $M\dot{V}O_2$ almost certainly underestimate "true" mitochondrial reserve capacity (the maximum capacity to support ATP utilization under physiological conditions). This is because decreases of the mitochondrial proton gradient also compromise important mitochondrial functions other than ATP synthesis such as maintenance of ion gradients; these functions are also required to support ATP synthesis (26). Consequently, DNP cannot be used estimate maximal $M\dot{V}O_2$ capacity (8). In intact tissues including myocardium, DNP can decrease the proton gradient to the point that the ATP synthesis rate required to support contractile and other cellular functions cannot be maintained despite a substantial increase in $M\dot{V}O_2$. However, it is reasonable to assume that a significant increase of $M\dot{V}O_2$ induced by DNP does indicate the presence of a reserve mitochondrial oxidative capacity so long as contractile function is maintained and HEP levels do not markedly deteriorate.

In summary, during the high workload produced by catecholamine stimulation, DNP was able to further increase $M\dot{V}O_2$ in compensated hypertrophied hearts, indicating a significant energy generation reserve. Furthermore, the increase of $M\dot{V}O_2$ in response to DNP occurred with no reduction of PCr/ATP. These findings support the view that primary abnormalities of oxidative ATP production did not constrain contractile performance at moderately high workloads in hearts with compensated pressure overload hypertrophy. In contrast, during catecholamine stimulation in failing hearts, DNP failed to increase of $M\dot{V}O_2$ and caused a significant reduction of PCr/ATP. These findings suggest that the capacity of some rate-limiting reaction(s) in the oxidative ATP synthetic pathway may have been reached during the high workload produced by catecholamine administration.

DISCLOSURES

This work was supported by National Heart, Lung, and Blood Institute Grants HL-50470, HL-61353, HL-67828, HL-71970, HL-33600, and HL-21872. J. Zhang was the recipient of an Established Investigator Award from the American Heart Association.

REFERENCES

1. **Bache RJ and Dai XZ.** Myocardial oxygen consumption during exercise in the presence of left ventricular hypertrophy secondary to supravalvular aortic stenosis. *J Am Coll Cardiol* 15: 1157–1164, 1990.
2. **Bache RJ, Zhang J, Murakami Y, Zhang Y, Cho YK, Merkle H, Gong G, From AHL, and Ugurbil K.** Myocardial oxygenation at high workstates in hearts with left ventricular hypertrophy. *Cardiovasc Res* 42: 616–626, 1999.
3. **Bache RJ, Zhang J, Path G, Merkel H, Hendrich K, From AH, and Ugurbil K.** High-energy phosphate responses to tachycardia and inotropic stimulation in left ventricular hypertrophy. *Am J Physiol Heart Circ Physiol* 266: H1959–H1970, 1994.
4. **Bishop SP and Altschuld RA.** Increased glycolytic metabolism in cardiac hypertrophy and congestive failure. *Am J Physiol* 218: 153–159, 1970.
5. **Chen W, Zhang J, Zhu XH, Zhang Y, Wang C, Merkle H, Eijgelshoven M, and Ugurbil K.** Determination of deoxymyoglobin changes of canine heart during partial and complete coronary artery occlusion using in vivo ^{1}H NMR spectroscopy. *Magn Reson Med* 38: 193–197, 1997.
6. **De Sousa E, Veksler V, Minajeva A, Kaasik A, Mateo P, Mayoux E, Hoerter J, Bigard X, Serrurier B, and Ventura-Clapier R.** Subcellular creatine kinase alterations Implications in heart failure. *Circ Res* 85: 68–76, 1999.
7. **Duncker DJ, Stubenitsky R, and Verdouw PD.** Autonomic control of vasomotion in the porcine coronary circulation during treadmill exercise: evidence for feed-forward beta-adrenergic control. *Circ Res* 29: 1312–1322, 1998.
8. **Elzinga G and van der Laarse WJ.** MVO_{2max} of the heart cannot be determined from uncoupled myocytes. *Basic Res Cardiol* 85: 315–317, 1990.
9. **From AH, Zimmer SD, Michurski SP, Mohanakrishnan P, Ulstad VK, Thoma WJ, and Ugurbil K.** Regulation of the oxidative phosphorylation rate in the intact cell. *Biochemistry* 29: 3731–3743, 1990.

10. **Hendrich K, Liu H, Merkle H, Zhang J, and Ugurbil K.** B_1 voxel shifting of phase-modulated spectroscopic localization techniques. *J Magn Reson* 97: 486–497, 1992.
11. **Hendrich K, Merkle H, Weisdorf S, Vine W, Garwood M, and Ugurbil K.** Phase modulated rotating frame spectroscopic localization using an adiabatic plane rotation pulse and a single surface coil. *J Magn Reson* 92: 258–275, 1991.
12. **Horn M, Neubauer S, Frantz S, Hugel S, Hu K, Gaudron P, Schnackerz K, and Ertl G.** Preservation of left ventricular mechanical function and energy metabolism in rats after myocardial infarction by the angiotensin-converting enzyme inhibitor quinapril. *J Cardiovasc Pharmacol* 27: 201–210, 1996.
13. **Jacob R and Gulch RW.** The functional significance of ventricular geometry for the transition from hypertrophy to cardiac failure. Does a critical degree of structural dilatation exist? *Basic Res Cardiol* 93: 423–429, 1998.
14. **Katz AM.** Is the failing heart energy depleted? *Cardiol Clin* 16: 633–644, 1998.
15. **Kingsley-Hickman P, Sako E, Foker J, From AHL, and Ugurbil K.** ^{31}P NMR measurements of mitochondrial uncoupling in isolated rat hearts. *J Biol Chem* 265: 1545–1550, 1990.
16. **Lawson JWR and Veech RL.** Effects of pH and free Mg^{2+} on the K_{eq} of the creatine kinase reaction and other phosphate hydrolyses and phosphate transfer reactions. *J Biol Chem* 254: 6528–6537, 1979.
17. **Liang CS and Hood WB Jr.** Comparison of cardiac output responses to 2,4-dinitrophenol-induced hypermetabolism and muscular work. *J Clin Invest* 52: 2283–2292, 1973.
18. **Liu J, Wang C, Murakami Y, Gong G, Ishibashi Y, Prody C, Ochiai K, Bache RJ, Godinot C, and Zhang J.** Mitochondrial ATPase and high-energy phosphates in failing hearts. *Am J Physiol Heart Circ Physiol* 281: H1319–H1326, 2001.
19. **Massie BM, Schaefer S, Garcia J, McKirnan D, Schwartz GG, Wisneski JA, Weiner MW, and White FC.** Myocardial high-energy phosphate and substrate metabolism in swine with moderate left ventricular hypertrophy. *Circulation* 91: 1814–1823, 1995.
20. **Mootha VK, Arai AE, and Balaban RS.** Maximum oxidative phosphorylation capacity of the mammalian heart. *Am J Physiol Heart Circ Physiol* 272: H769–H775, 1997.
21. **Murakami Y, Zhang J, Eijgelshoven MH, Chen W, Carlyle WC, Zhang Y, Gong G, and Bache RJ.** Myocardial creatine kinase kinetics in hearts with postinfarction left ventricular remodeling. *Am J Physiol Heart Circ Physiol* 276: H892–H900, 1999.
22. **Neubauer S, Horn M, Cramer M, Harre K, Newell JB, Peters W, Pabst T, Ertl G, Hahn D, Ingwall JS, and Kochsiek K.** Myocardial phosphocreatine-to-ATP ratio is a predictor of mortality in patients with dilated cardiomyopathy. *Circulation* 96: 2190–2196, 1997.
23. **Neubauer S, Horn M, Naumann A, Tian R, Hu K, Laser M, Friedrich J, Gaudron P, Schnackerz K, Ingwall JS, and Ertl G.** Impairment of energy metabolism in intact residual myocardium of rat hearts with chronic myocardial infarction. *J Clin Invest* 95: 1092–1100, 1995.
24. **Ning XH, Zhang J, Liu J, Ye Y, Chen SH, From AH, Bache RJ, and Portman MA.** Signaling and expression for mitochondrial membrane proteins during left ventricular remodeling and contractile failure after myocardial infarction. *J Am Coll Cardiol* 36: 282–287, 2000.
25. **Port JD and Bristow MR.** Altered beta-adrenergic receptor gene regulation and signaling in chronic heart failure. *J Mol Cell Cardiol* 33: 887–905, 2001.
26. **Ravesloot JH and Rombouts E.** 2,4-Dinitrophenol acutely inhibits rabbit atrial Ca^{2+}-sensitive Cl^- current (I_{TO2}). *Can J Physiol Pharmacol* 78: 766–773, 2000.
27. **Robitaille PM, Lew B, Merkle H, Path G, Sublett E, Hendrich K, Lindstrom P, From AHL, Garwood M, Bache RJ, and Ugurbil K.** Transmural high energy phosphate distribution and response to alterations in workload in the normal canine myocardium as studied with spatially localized ^{31}P NMR spectroscopy. *Magn Reson Med* 16: 91–116, 1990.
28. **Robitaille PM, Lew B, Merkle H, Sublett E, Lindstrom P, From AHL, Garwood M, Bache RJ, and Ugurbil K.** Transmural metabolite distribution in regional myocardial ischemia as studied with ^{31}P NMR. *Magn Reson Med* 10: 108–118, 1989.
29. **Robitaille PM, Merkle H, Sublett E, Hendrich K, Lew B, Path G, From AHL, Bache RJ, and Ugurbil K.** Spectroscopic imaging and spatial localization using adiabatic pulses and applications to detect transmural metabolite distribution in the canine heart. *Magn Reson Med* 10: 14–37, 1989.
30. **Scott JC, Gold M, Bechtel AA, and Spitzer JJ.** Influence of 2,4-dinitrophenol on myocardial metabolism and hemodynamics. *Metabolism* 17: 370–376, 1968.
31. **Sellevold OFM, Jynge P, and Aartad K.** High performance liquid chromatography: a rapid isocratic method for determination of creatine compounds and adenosine nucleotides in myocardial tissue. *J Mol Cell Cardiol* 18: 517–527, 1986.
32. **Sharov VG, Goussev A, Lesch M, Goldstein S, and Sabbah HN.** Abnormal mitochondrial function in myocardium of dogs with chronic heart failure. *J Mol Cell Cardiol* 30: 1757–1762, 1998.
33. **Sordahl LA, McCollum WB, Wood WG, and Schwartz A.** Mitochondria and sarcoplasmic reticulum function in cardiac hypertrophy and failure. *Am J Physiol* 224: 497–502, 1973.
34. **Towbin JA and Bowles NE.** Molecular genetics of left ventricular dysfunction. *Curr Mol Med* 1: 81–90, 2001.
35. **Ye Y, Gong G, Ochiai K, Liu J, and Zhang J.** High-energy phosphate metabolism and creatine kinase in failing hearts: a new porcine model. *Circulation* 103: 1570–1576, 2001.
36. **Zhang J and McDonald KM.** Bioenergetic consequences of left ventricular remodeling. *Circulation* 92: 1011–1019, 1995.
37. **Zhang J, Merkle H, Hendrich K, Garwood M, From AHL, Ugurbil K, and Bache RJ.** Bioenergetic abnormalities associated with severe left ventricular hypertrophy. *J Clin Invest* 92: 993–1003, 1993.
38. **Zhang J, Murakami Y, Zhang Y, Cho YK, Ye Y, Gong G, Bache RJ, Ugurbil K, and From AHL.** Oxygen delivery does not limit cardiac performance during high work states. *Am J Physiol Heart Circ Physiol* 277: H50–H57, 1999.
39. **Zhang J, Wilke N, Wang Y, Zhang Y, Wang C, Eijgelshoven MH, Cho YK, Murakami Y, Ugurbil K, Bache RJ, and From AHL.** Functional and bioenergetic consequences of postinfarction left ventricular remodeling in a new porcine model. MRI and ^{31}P-MRS study. *Circulation* 94: 1089–1100, 1996.